Confinement of band-edge modes in a photonic crystal slab

Frédéric Bordas,[1] **M. J. Steel,**[2,3] **Christian Seassal,**[1] **Adel Rahmani**[4]

[1] *Université de Lyon, Institut des Nanotechnologies de Lyon INL-UMR5270, CNRS, Ecole Centrale de Lyon, Ecully, F-69134, France*
[2] *RSoft Design Group, Inc., 65 O'Connor Street, Chippendale, NSW 2008, Australia*
[3] *Centre for Ultrahigh-bandwidth Devices for Optical Systems (CUDOS), School of Physics, University of Sydney, NSW 2006,Australia*
[4] *Centre for Ultrahigh-bandwidth Devices for Optical Systems (CUDOS), Department of Physics, Macquarie University, NSW 2109, Australia*

Frederic.Bordas@ec-lyon.fr

Abstract: We study the confinement of low group velocity band-edge modes in a photonic crystal slab. We use a rigorous, three dimensional, finite-difference time-domain method to compute the electromagnetic properties of the modes of the photonic structures. We show that by combining a defect mode approach with the high-density of states associated with band-edge modes, one can design compact, fabrication-tolerant, high-Q photonic microcavities. The electromagnetic confinement properties of these cavities can foster enhanced radiation dynamics and should be well suited for ultralow-threshold microlasers and cavity quantum electrodynamics.

OCIS codes: (230.3990) Microstructure devices; (230.5750) Resonators; (140.5960) Semiconductor lasers

References and links

1. E. Yablonovitch, "Inhibited spontaneous emission in solid-state physics and electronics," Phys. Rev. Lett. **58**, 2059-2062 (1987).
2. S. John, "Strong localization of photons in certain disordered dielectric superlattices," Phys. Rev. Lett. **58**, 2486-2489 (1987).
3. J. D. Joannopoulos, R. D. Meade, J. N. Winn, "Photonic Crystals: Molding the Flow of Light" (Princeton, 1995).
4. K. Sakoda, "Optical Properties of Photonic Crystals," 2nd edition (Springer, 2004).
5. Y. Akahane, T. Asano, B. -S. Song, and S. Noda, "Fine-tuned high-Q photonic-crystal nanocavity," Opt. Express **13**, 1202-1214 (2005), http://www.opticsexpress.org/abstract.cfm?id=82669.
6. A. M. Yacomotti, P. Monnier, F. Raineri, B. Ben Bakir, C. Seassal, R. Raj, and J. A. Levenson, "Fast Thermo-Optical Excitability in a Two-Dimensional Photonic Crystal," Phys. Rev. Lett. **97**, 143904 (2006).
7. C. Monat, C. Seassal, X. Letartre, P. Regreny, P. Rojo-Romeo, P. Viktorovitch, M. Le Vassor d'Yerville, D. Cassagne, J. P. Albert, E. Jalaguier, S. Pocas, and B. Aspar, "InP-based two-dimensional photonic crystal on silicon: In-plane Bloch mode laser," Appl. Phys. Lett. **81**, 5102-5104 (2002).
8. B. Ben Bakir, C. Seassal, X. Letartre, P. Viktorovitch, M. Zussy, L. Di Cioccio, and J. M. Fedeli, "Surface-emitting microlaser combining two-dimensional photonic crystal membrane and vertical Bragg mirror," Appl. Phys. Lett. **88**, 081113 (2006).
9. K. Srinivasan and O. Painter, "Fourier space design of high-Q cavities in standard and compressed hexagonal lattice photonic crystals," Opt. Express **11**, 579-593 (2003), http://www.opticsexpress.org/abstract.cfm?id=71672.
10. Kartik Srinivasan, Paul E. Barclay and Oskar Painter, "Fabrication-tolerant high quality factor photonic crystal microcavities," Opt. Express **12**, 1458-1463 (2004), http://www.opticsexpress.org/abstract.cfm?id=79471.
11. http://www.rsoftdesign.com
12. O. Painter, K. Srinivasan, and P.E. Barclay, "A Wannier-like Equation for Localized Resonant Cavity Modes of Locally Perturbed Photonic Crystals," Phys. Rev. B, **68**, 035214 (2003).

#82387 - $15.00 USD Received 24 Apr 2007; revised 11 Jun 2007; accepted 11 Jun 2007; published 15 Aug 2007

13. O. Painter, K. Srinivasan, "Localized defect states in two-dimensional photonic crystal slab waveguides: a simple model based upon symmetry analysis," Phys. Rev. B, **68**, 035110 (2003).
14. C. Sauvan, G. Lecamp, P. Lalanne, and J. P. Hugonin, "Modal-reflectivity enhancement by geometry tuning in Photonic Crystal microcavities," Opt. Express **13**, 245-255 (2005), http://www.opticsinfobase.org/abstract.cfm?URI=oe-13-1-245
15. C. Sauvan, P. Lalanne, and J. P. Hugonin, "Slow-wave effect and mode-profile matching in photonic crystal microcavities," Phys. Rev. B **71**, 165118 (2005)
16. V. A. Mandelshtam and H. S. Taylor, "Harmonic inversion of time signals," J. Chem. Phys. **107**, 6756-6769 (1997). Erratum, ibid. 109 (10), 4128 (1998).
17. Y. Akahane, T. Asano, B.-S. Song, and S. Noda, "High-Q photonic nanocavity in a two-dimensional photonic crystal," Nature **425**, 944-947 (2003)
18. Soon-Hong Kwon, Se-Heon Kim, Sun-Kyung Kim and Yong-Hee Lee, "Small, low-loss heterogeneous photonic bandedge laser," Opt. Express **12**, 5356-5361 (2004), http://www.opticsexpress.org/abstract.cfm?id=81633.
19. K. Srinivasan and O. Painter, "Momentum space design of high-Q photonic crystal optical cavities," Opt. Express **10**, 670-684 (2002), http://www.opticsinfobase.org/abstract.cfm?URI=oe-10-15-670
20. A. Rahmani and P. C. Chaumet, "Optical trapping near a photonic crystal," Opt. Express **14**, 6353-6358 (2006), http://www.opticsinfobase.org/abstract.cfm?URI=oe-14-13-6353
21. M. Barth and O. Benson, "Manipulation of dielectric particles using photonic crystal cavities," Appl. Phys. Lett. **89**, 253114 (2006)

1. Introduction

Photonic crystal (PC) structures have allowed an unprecedented level of control of light in space, frequency, and time [1–4]. The two major strategies when designing PC slab devices are the introduction of defects, and the exploitation of the critical points of the band dispersion diagram of the perfect crystal. The former approach creates a defect state in the photonic band gap, the defect constituting a cavity for photons. However, these cavities often draw their properties of confinement from an astute management of losses which relies on the careful control of the optical reflections at the boundaries of the cavity. This means that the fabrication of such structures often requires minute adjustments to the structure of the crystal [5].

The second approach considers the perfect crystal (without defects) and builds upon the enhanced local density of electromagnetic states associated with the critical points of the band dispersion diagram. Near these points, the slope of the band is very small and the crystal supports slow light modes (SLMs). Owing to their small group velocity, SLMs are associated with a stronger local density of electromagnetic states than conventional modes with a larger group velocity. This property makes SLMs an asset in achieving enhanced nonlinear effects [6] or low threshold laser emission [7, 8]. However, the main drawback of the modes of a defect-free crystal is that they are spatially delocalized. This leads to practical problems in the design of compact photonic microstructures. It also implies a more fundamental problem, if the mode size is only limited by its losses, or alternatively, if a large quality factor requires a large photonic crystal structure, how can one design a structure exploiting band-edge SLMs with a high ratio of the quality factor Q to the mode volume V, necessary to foster enhanced radiation dynamics? Srinivasan and coworkers have shown that a band-edge mode could be confined effectively using a graded lattice [9, 10]. In particular they studied the symmetry and Fourier-space properties of such modes. In a related, but different approach, starting from the *delocalized* band-edge mode of a PC slab, we are interested in finding out how, or if, the lateral size of the mode can be reduced without introducing drastic losses. We present a systematic study of the confinement of a band-edge mode in a PC slab with a discussion of spatial versus temporal confinement. We show that band-edge SLMs can be confined spatially without incurring drastic losses. In particular, we show that a high ratio of the quality factor to the field mode volume can be achieved by confining valence band-edge modes, leading to PC designs that provide a suitable platform for cavity-quantum electrodynamics experiments and low-threshold lasing.

#82387 - $15.00 USD Received 24 Apr 2007; revised 11 Jun 2007; accepted 11 Jun 2007; published 15 Aug 2007

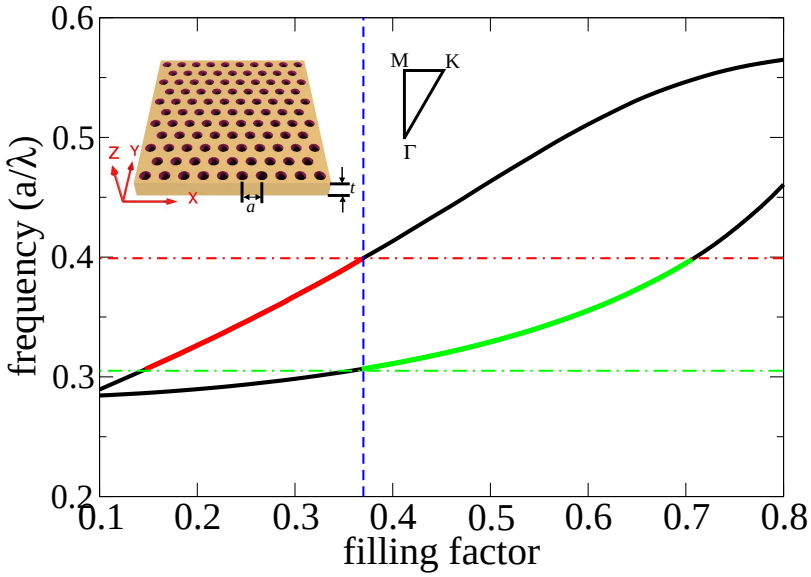

Fig. 1. Frequency of the band-edges versus the filling factor for a PC slab. a is the period of the crystal and λ is the wavelength of the mode. The vertical dashed line corresponds to a crystal with a filling factor $f = 0.37$. The horizontal dash-dotted lines mark the band edges of a crystal with $f = 0.37$. Insets: Lattice geometry of the photonic crystal slab and location of main symmetry points in the first Brillouin zone.

2. Concept

Our PC geometry consists of a semiconductor slab (Indium Phosphide with refractive index n=3.17), surrounded by air, and patterned with a triangular array of air holes (Fig. 1, inset). The period of the lattice is a, the thickness of the slab is $t = 11a/26$, and the air filling factor is $f = 2\pi/\sqrt{3}(r/a)^2$, where r is the radius of the air holes. We consider modes that are even with respect to a mirror plane passing through the center of the slab (TE-like modes). For these modes, the chosen geometry has a bandgap between the first and the second band. The edge of the valence (first) band is at the K point of the first Brillouin zone (BZ), whereas the edge of the conduction (second) band lies at M. Figure 1 gives the frequency of the two band edges as a function of f computed by 3D plane wave expansion [11]. As shown in Fig. 1, one can tune the position of the band edges by changing f. If, for instance, we consider a PC with $f = 0.37$ (vertical dashed line in Fig. 1), we see that its bandgap lies between a/λ =0.307 and a/λ =0.400. Figure 1 suggests that a second PC with the same lattice parameter, and $0.37 < f < 0.7$ would have its valence band edge in the bandgap of the first PC. Similarly, a PC with $0.15 < f < 0.37$ would have its conduction band edge lying in the band gap of the first PC. These ideas relate to the concepts of donor (valence) and acceptor (conduction) defect modes described in detail by Painter and coworkers [12, 13].

In this article we seek to explore the influence of the size of the "defect" area on the spatial and energy confinement of the band-edge mode. This will also give us an insight in the evolution of a band-edge mode as it becomes confined. We shall focus on valence modes, for which light is mostly in the high-index material, thereby ensuring optimal interaction with sources that would be inside the slab. We will show that this approach leads to cavity designs with a large Q/V ratio.

#82387 - $15.00 USD Received 24 Apr 2007; revised 11 Jun 2007; accepted 11 Jun 2007; published 15 Aug 2007

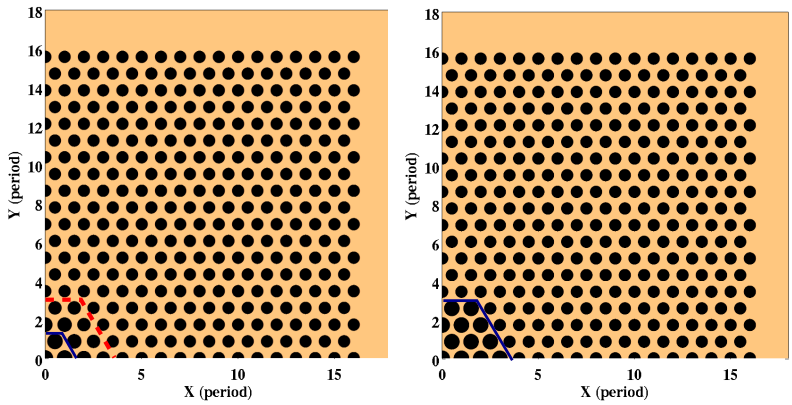

Fig. 2. Examples of structures: V_2^2 cavity (left) and V_4^0 cavity (right). Only the top-right quadrant (2D projection of one octant of the computational window) is shown. The core has a hexagonal shape, with a higher air filling factor than the mirror ($f_{\text{mirror}} = 0.37$). Hexagonal rings of intermediary hole radii can be used to soften the transition from the core to the mirror region.

3. Geometry of the photonic crystal structure

We consider a finite PC slab, with $f = f_{\text{mirror}} = 0.37$ comprising 33 and 37 rows of holes along directions x and y respectively. This gives us a crystal that is large enough for us to study cavities with different lateral dimensions, while keeping an overall structure of a practical size. At the center of this structure we modify the radius of i hexagonal rings of holes to make them bigger (*i.e.*, the filling factor of the central region $f_{\text{core}} > f_{\text{mirror}}$). Furthermore, we anticipate that the abrupt transition between core and mirror regions will lead to out-of-plane scattering losses. Therefore, we allow a linear variation of the radius of the holes from the core to the cladding across an additional j hexagonal adaptation rings. We will refer to this cavity as V_i^j, as it supports valence band edge modes. Of course, a cavity with a core consisting of a single hole and a large number of adaptation layers would yield the graded-lattice design of Srinivasan et al. [9, 10, 12].

Figure 2 shows the upper-right quadrant of the in-plane computational domain for two examples of cavities. We use symmetry conditions to reduce the computational domain by a factor of 8. We use a commercial, parallel implementation of the three-dimensional finite-difference time-domain (FDTD) method to solve rigorously Maxwell's equations for the PC structures [11]. The modal fields, resonant frequency ν, and quality factor Q are found by a sequence of FDTD runs. From an initial FDTD run with a localized Gaussian excitation, estimates of the resonant frequency ν and Q factor are calculated using the filter diagonalization method [16]. The calculation is then repeated and the modal field is extracted by discrete Fourier transform at the approximate frequency ν. This process is repeated a number of times with successively longer computation times to refine the modal frequency and spatial profile until the results are converged. Properties such as in-plane ($Q_{\parallel}$) and out-of-plane ($Q_{\perp}$) quality factors are found by post-processing the fields (see Appendix). An interesting property of these structures is that a good estimate of the quality factor Q of the mode can be obtained with a coarse spatial discretization grid. Indeed, computations with a spatial grid of $a/16$ typically yield an estimate of Q within 10-15%, and sometimes even within a few percent of the results obtained with a higher spatial sampling rate ($\Delta x = a/32$). It is therefore possible to find a good

#82387 - $15.00 USD Received 24 Apr 2007; revised 11 Jun 2007; accepted 11 Jun 2007; published 15 Aug 2007

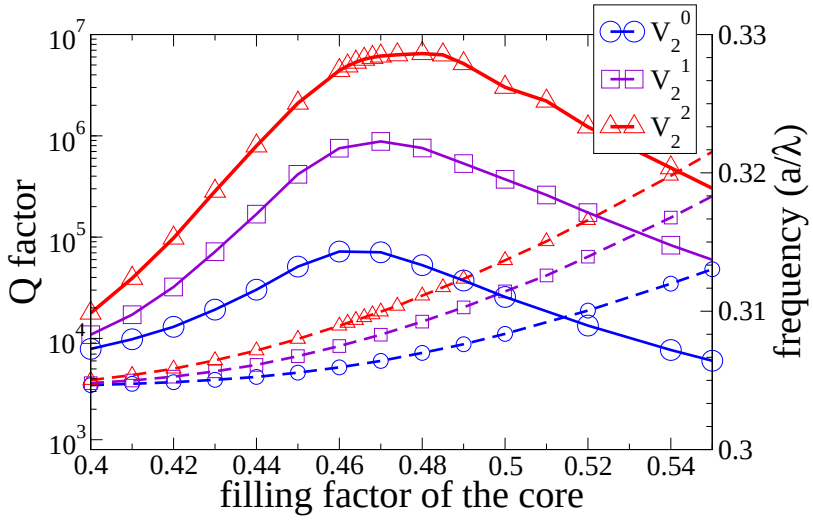

Fig. 3. Quality factor Q (solid lines) and frequency (dashed lines) of the confined band-edge mode versus the filling factor of the core for V_2^j cavities with j=0, 1, 2.

compromise between the speed and the accuracy of the computation. The plots presented in this article were calculated with a cell size of $\Delta x = a/16$.

From a physical point of view, the low sensitivity of the mode with respect to the numerical discretization relates to the fact that, unlike in some other designs where the spatial confinement properties of the mode are governed by the scattering of the field associated with the mode at one or two holes, in the present design, the mode is "distributed" over several lattice sites. This yields a design that is robust with respect to lattice imperfection. This was also pointed out by Srinivasan and coworkers in their study of a conduction (donor) band-edge mode confined by a graded lattice [10]. Furthermore, we shall see that this type of design is also robust with respect to *systematic* fabrication errors.

4. Influence of the adaptation layers

Figure 3 shows the evolution of Q and normalized frequency $\nu = a/\lambda$ versus the filling factor of the core, for the valence band-edge mode of V_2^j cavities. We consider modes with an even and odd symmetry with respect to mirror reflection through the (x,z) and (y,z) planes, respectively (note that there exist also a mode with even-even symmetry). For the V_2^0 structure, which corresponds to a core with 2 rings of holes (7 holes in total) surrounded by the mirror region, we see that the quality factor of the core mode has a maximum of 7×10^4 at $f_{\text{core}} = 0.46$. The frequency of the mode, on the other hand, increases monotonically with f_{core}. We emphasize that the maximum of Q, which corresponds to the optimal electromagnetic temporal confinement, does not occur when the frequency of the mode is at the center of the bandgap, but actually quite close to the valence band edge of the mirror PC. (Note that the mode must lie between the solid and dotted green lines in Fig. 1.) We shall get back to this point later.

If we soften the transition between core and mirror regions using 1 or 2 adaptation layers, we observe a similar evolution of $Q(f)$ except that the quality factor increases significantly, reaching a maximum around 5.5×10^6 (computed with $\Delta x = a/32$) for $f_{\text{core}} = 0.48$ with 2 adaptation layers (Fig. 3). Thus, even one or two adaptation layers enables a significant increase in Q. What is perhaps even more interesting is that the increase in mode volume experienced

#82387 - $15.00 USD Received 24 Apr 2007; revised 11 Jun 2007; accepted 11 Jun 2007; published 15 Aug 2007

by the SLM, as more adaptation layers are introduced, is slow enough to ensure that Q/V increases with the number of layers. However, as the number of adaptation layer is increased, the variation of the radius of the holes between two adjacent adaptation layers becomes smaller, thereby making the structure more difficult to fabricate. Therefore, the use of two adaptation layers seems like a convenient trade-off between increasing the quality factor of the cavity, and keeping the fabrication process as simple as possible.

5. Energy *vs.* spatial confinement

Before looking at the confinement properties of various cavity geometries let us consider a particular design and use it to gain some insight into the electromagnetic processes that govern the confinement of light in this type of cavity.

The optical properties of these cavities are the result of the balance between two effects: mode spatial confinement, which is *maximal* for large filling factors (when the band-edge mode of the core lies deep inside the bandgap of the mirror region), and lattice-mismatch (and by extension mode-mismatch [14]), which is *minimal* when f_{core} is close to f_{mirror}. In other words, starting from $f_{\text{core}} = f_{\text{mirror}}$, as f_{core} increases, Q starts to increase because the mode confinement is improved and *in-plane* losses (IPL) are reduced. The quality factor then reaches a maximum and starts decreasing due to a stronger lattice mismatch which results in stronger *out-of-plane* losses (OPL). The large quality factors obtained for these cavities is also consistent with the analysis presented in [15] which emphasized that a good optical confinement can be achieved through a combination of slow-light (the band-edge mode of the core in our case) and mode-matching at the boundary of the cavity (use of adaptation layers).

To explore the interplay between in-plane and out-of-plane losses, we plot in Fig. 4 the quality factor and mode volume of the core mode versus the filling factor for the V_2^2 cavity. We see that the spatial confinement of the mode is maximal for large values of f_{core} and that the maximum of Q does not coincide with the optimal spatial confinement of the mode. This is a

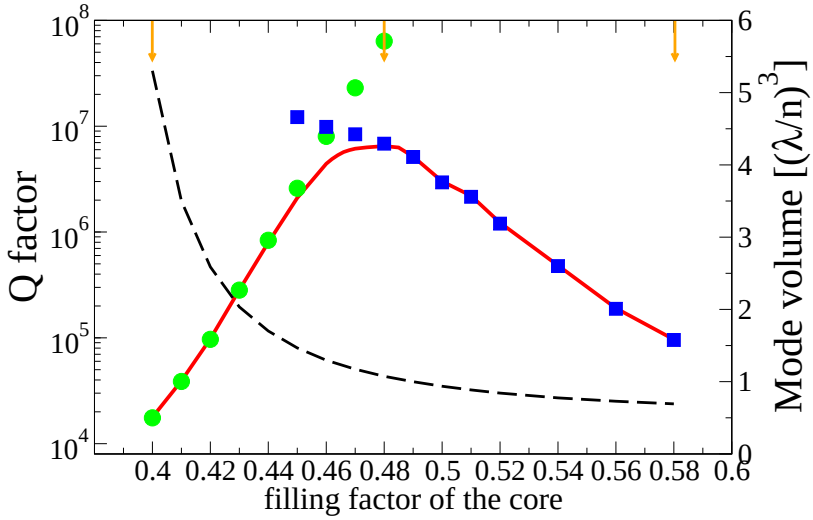

Fig. 4. Quality factor (solid line) and mode volume (dashed line) versus core filling factor for a V_2^2 cavity. The circles and squares represent the in-plane, and out-of-plane quality factors, respectively. The arrows at the top of the graph indicate the filling factors for which the field maps in Fig. 5 were computed.

#82387 - $15.00 USD Received 24 Apr 2007; revised 11 Jun 2007; accepted 11 Jun 2007; published 15 Aug 2007

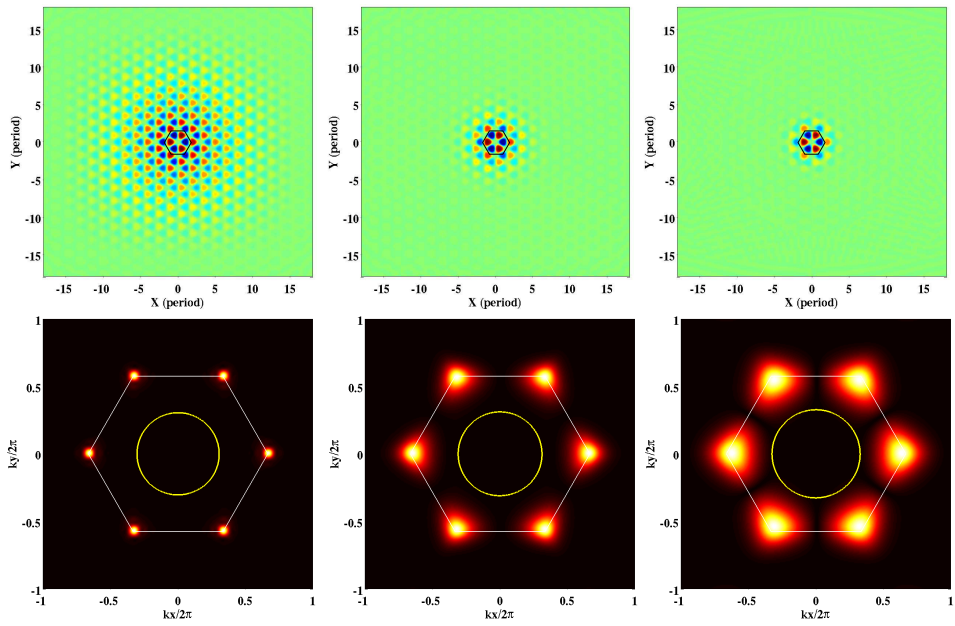

Fig. 5. Near-field map of H_z (top row) and $|\mathscr{F}(H_z)|$ (bottom row) for the V_2^2 cavity. From left to right, the columns correspond to the values of the filling factor marked on Fig. 3 (f=0.40, 0.48, and 0.58, respectively). On the real-space plots, the black hexagon delineates the core region. On the FFT plots, the white hexagon outlines the boundary of the first Brillouin zone and the yellow circle materializes the boundary of the light cone

consequence of the three-dimensional nature of the structure and relates to out-of-plane losses. This is confirmed by an analysis of the separate contributions from in-plane and out-of-plane losses to the quality factor (Fig. 4). It is clear that $Q_{\parallel}$ increases as the mode moves deeper into the band gap, while $Q_{\perp}$ decreases as the lateral confinement of the mode improves.

Another illustration of the effect of confinement can be seen in Fig. 5 where we plot the near-field maps of the $z-$component of the magnetic field H_z above the slab, and its Fourier transform $|\mathscr{F}(H_z)|$, for the three values of f_{core} marked by arrows in Fig. 4. For $f_{\text{core}} = 0.40$ the mode is fairly delocalized because the SLM in the core is close to the band-edge of the mirror region which behaves like a weak mirror. In other words, the SLM is in a weak potential well and its evanescent tail decays very slowly outside of the core. On the other hand, the Fourier space plot shows that the mode spectral signature consists of a well confined peak around the K points of the first BZ (with a much weaker contribution from the equivalent symmetry points outside the first BZ which are not shown). As f_{core} increases (Fig. 5), the SLM experiences a tighter confining potential, which results in a highly confined mode profile that almost coincides with the physical size of the core. In Fourier space, however, the peaks at the K points of the first BZ experience a strong broadening and start to leak into the light cone (whose projection is represented by a circle in Fig. 5), thereby causing an increase of out-of-plane losses [17] and the decrease in $Q_{\perp}$ seen in Fig. 4. Incidentally, the fact that the spectral components of the core mode are quite far away from the light cone suggest that these structures are relatively independent of the substrate index, and could still support a mode with a fairly large quality factor with different implementations, as silicon on insulator, or InP bonded to a dielectric substrate.

#82387 - $15.00 USD Received 24 Apr 2007; revised 11 Jun 2007; accepted 11 Jun 2007; published 15 Aug 2007

6. Influence of the size of the core on the confinement

We have established that the optical properties of the cavity-confined band-edge mode are the result of a balance between IPL and OPL. Having also described the effect of adaptation layers on the confinement of the mode, we now study the influence of the size of the core on the confinement of the SLM.

We consider cavities with a core consisting of 1 up to 5 rings of holes. To emphasize the role of the size of the core, all cavities have the same number of adaptation layers (2). Figure 6 presents the evolution of the quality factor versus the filling factor of the core for all these cavities. For $f_{\text{core}} \lessapprox 0.43$ the quality factor increases with the size of the core. In first approximation, this reflects the mere fact that the bigger the core of the cavity, the longer it takes for photons to undergo successive "bounces" off the edges of the cavity where out-of-plane scattering occurs.

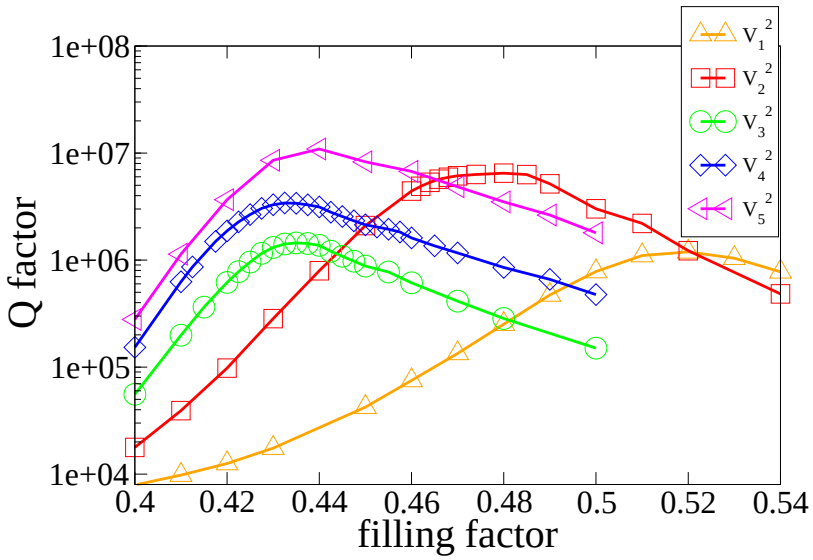

Fig. 6. Quality factor Q of the confined slow-light mode vs. filling factor of the core for V_i^2 cavities with $i = 1,2,3,4,5$.

One can notice the similar evolution of the $Q(f)$ curves for the V_3^2, V_4^2, and V_5^2 cavities on Fig. 6. The three curves have their maximum at about the same filling factor, and the slopes are comparable. The only difference comes from the values of Q, which are higher for a larger core, as more energy is stored within the cavity.

Perhaps less trivial is the difference in behavior of the V_1^2 and V_2^2 cavities compared to cavities with a bigger core. These differences can be explained on the basis of Fig. 7 and the interpretation presented in the previous section. As the core gets bigger, the frequency of the mode of the core moves closer to the frequency of the valence band-edge of an infinite crystal with $f = f_{\text{core}}$ (Fig. 7). Furthermore, because the frequency of the confined SLM increases more rapidly with f_{core} for larger sizes of the core, the confined SLM moves across the bandgap of the mirror PC over a shorter range of values of f_{core}, leading to a wider "bandwidth" for the cavities with a small core (Fig. 7). As a consequence, the V_2^2, for instance, exhibits a large quality factor ($> 10^6$) over a large range of values of filling factors. This is an interesting property as it ensures that the quality factor will be fairly insensitive to a moderate systematic fabrication error (e.g., lithographic or etching process yielding holes systematically smaller or

#82387 - $15.00 USD Received 24 Apr 2007; revised 11 Jun 2007; accepted 11 Jun 2007; published 15 Aug 2007

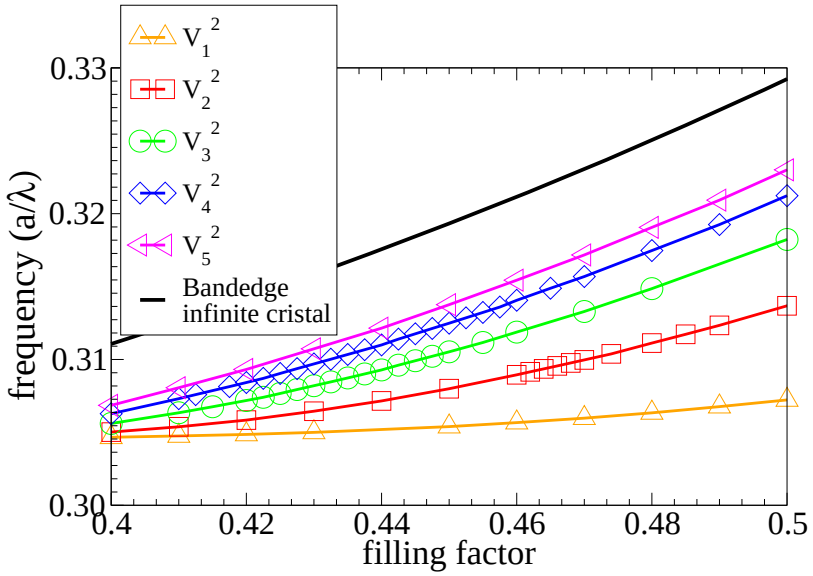

Fig. 7. Frequency of the confined slow-light mode vs. filling factor of the core for V_i^2 cavities with $i = 1,2,3,4,5$. The solid line without symbols represents the valence band-edge for a perfect (infinite) crystal.

larger than the optimal, computed filling factor).

Therefore, for a small-core cavity, the filling factor has to reach a larger value before the core mode is deep inside the bandgap of the mirror PC, stage at which OPL becomes the dominant loss mechanism. This explains why the highest quality factor corresponds to a larger filling factor of the core as the core gets smaller. The location of the maximum of $Q(f)$ does not vary much between the V_3^2, V_4^2 and V_5^2 cavities because the mode starts to experience the influence of the finite size of the mirror PC. Indeed, because the size of the PC structure is the same for all cavities, the effective mirror size is smaller for a bigger core size. This explains why the evolution of the quality factor versus the size of the core does not follow the same trend once the core has reached a certain size (3 rings of holes in our example). Additional calculations (not reported here) show that with a wider mirror PC, the part of the $Q(f)$ curves to the left of the maximum is shifted upward whereas the part to the right of the maximum remains unchanged. As a consequence the maximum value of Q is reached at a smaller filling factor. This is a mere consequence of the reduction of the IPL resulting from the introduction of a wider mirror.

We can also take a closer look at the evolution of the mode volume for cavities of different core size (Fig. 8). While the general trend is the same for all cavities, *ie.*, the volume of the mode shrinks as the cavity moves deeper into the bandgap of the surrounding PC, we observe that the size of the core has an impact on how well the mode can ultimately be confined. For small filling factors the mode is highly delocalized and the mode volume is somewhat difficult to quantify as the mode is artificially truncated at the boundaries of the simulation window. On the other hand, as the mode moves deeper into the bandgap and its lateral size is reduced, a comparison of the mode volumes for the different cavities becomes meaningful. Perhaps the most interesting point is that deep in the bandgap, it is not the V_1^2 but the V_2^2 design that yields the smallest mode volume. This illustrates once again the complex interplay between IPL and OPL. In that sense the V_2^2 represents the best compromise between lateral spatial confinement

#82387 - $15.00 USD Received 24 Apr 2007; revised 11 Jun 2007; accepted 11 Jun 2007; published 15 Aug 2007

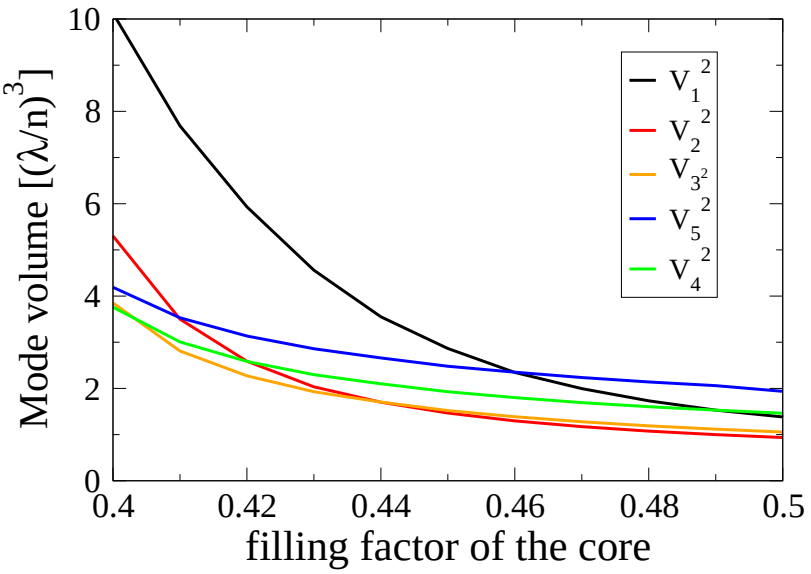

Fig. 8. Normalized mode volume of the confined slow-light mode vs. filling factor of the core for V_i^2 cavities with $i = 1,2,3,4,5$.

and vertical radiation losses.

7. Conclusion

We have demonstrated the possibility to confine band-edge, slow-light modes within a cavity in a photonic crystal slab. We have described the physical processes that govern the dynamics of these modes, and we have shown that the optical properties of these cavities result from an interplay between band-gap confinement and lattice mismatch. The designs that emerge from this study should yield resilient, fabrication-tolerant, two-dimensional slow-light modes. Indeed, large quality factors can be achieved over a wide range of hole sizes which ensures a high tolerance with respect to systematic fabrication errors. Furthermore, we observed that within these structures, the confinement of the mode is fairly impervious to the coarseness of the FDTD discretization grid. This points toward the possibility of designing PC structures that would be robust with respect to random fabrication errors as well [10]. Owing to their ability to direct very efficiently photon emission from a source located at the center of the slab into a mode with a large Q/V ratio, these cavities will be ideal for low-threshold lasing and cavity quantum electrodynamics. In fact, a particular case (V_3^0) of this class of band-edge cavities has already been used to demonstrate room-temperature lasing using multiple quantum wells as gain material [18]. The present work shows that spatially confined band-edge modes should be able to support low-threshold lasing even with less gain material, such as with a low density distribution of quantum dots instead of multiple quantum wells. Finally, we note that while the confined valence modes create an evanescent field above the slab which might be interesting for optical sensing the present approach can also be applied to conduction band-edge modes. In particular, using a larger core region might increase the quality factor without increasing drastically the mode volume compared to a graded lattice approach [9, 19]. Moreover, since for conduction modes the electromagnetic energy lies mostly in the holes, they might be more suitable for optical sensing and optical trapping [20, 21]. This is particularly interesting since

#82387 - $15.00 USD Received 24 Apr 2007; revised 11 Jun 2007; accepted 11 Jun 2007; published 15 Aug 2007

further calculations suggest that, using the present approach, large quality factors should be achievable with materials with a refractive index lower than those of common semiconductors.

We thank Dr. Badhise Ben Bakir, Dr. Christelle Monat and Prof. Martijn de Sterke for many useful discussions.

This work was supported by the Ministère délégué à la Recherche et aux Nouvelles Technologies (Programs "ACI Jeune Chercheur" and "ACN Nanoqub"), by the Australian Research Council Centres of Excellence and Linkage International Fellowship schemes and by an award under the Merit Allocation Scheme on the National Facility of the Australian Partnership for Advanced Computing.

A. Details on the numerical procedures for the FDTD calculation

Once the modal fields have been found using sequences of FDTD runs and application of the filter diagonalization method [16], we extract other parameters by post-processing of this data.

- The modal volume
$$V = \frac{\int \mathrm{d}\mathbf{r}^3 U_e(\mathbf{r})}{\max[U_e]},$$
is found by direct integration of the electric energy $U_e(\mathbf{r}) = \varepsilon(\mathbf{r})|\mathbf{E}(\mathbf{r})|^2/2$ and expressed in units of $(\lambda/n)^3$, where n is the refractive index of the slab.

- The in-plane $Q_{\parallel}$ and out-of-plane $Q_{\perp}$ quality factors are found by time-averaging of the directly measured integrated Poynting fluxes through planes at $x = 17a$, $y = 17a$ and $z \approx t/2 + \lambda/4$ (where λ is the wavelength of the mode), while the converged mode is allowed to decay for one or more additional periods. In certain parts of the parameter space where $Q_{\perp}$ is very large, the mean out-of-plane flux is dwarfed by the oscillatory flux of the evanescent near-field. This produces large uncertainties in the value of $Q_{\perp}$. This can be alleviated by longer propagation times to produce better time-averages, or by measuring the flux at a cut-plane of larger z, where the evanescent field is weaker. As $Q_{\perp}$ continues to rise beyond 10^7, the only solution would be to use a larger domain in the vertical direction to guarantee that the evanescent field was very weak, which would seriously increase the required simulation time. Since in these ranges, however, the cavity loss is dominated by the in-plane loss, the precise value of $Q_{\perp}$ ceases to be important. Another problem with choosing a measurement plane at large z is that at the other end of the parameter range, where $Q_{\perp}$ becomes quite low, the angular spread of the radiation becomes quite large. Therefore choosing a measurement plane far from the surface of the slab would result in a significant proportion of the vertically-emitted energy being incorrectly classified as in-plane losses. Ultimately, the choice of cut-planes and the division into in-plane and out-of-plane losses is somewhat arbitrary. It is the changes in these quantities with variation in the structure that contains the important physics.

Before commencing our parameter space analysis, we performed a thorough convergence study with respect to the following numerical parameters:

- The width of the perfectly matched layer boundaries was set to $w_{\mathrm{PML}} = a$ and $w_{\mathrm{PML}} = 2a$.

- The grid size was varied over the values Δx = $a/12$, $a/16$, $a/20$, $a/24$, $a/32$ with the other grid sizes given by $\Delta y = \sqrt{3}/2\Delta x$, $\Delta z = (t/2)/\mathrm{round}(t/2\Delta x)$.

- The distance to the simulation boundary above the plane was varied over the values $z_{\max}$ = 1.5a, 2.0a, 2.5a, 3.0a.

#82387 - $15.00 USD Received 24 Apr 2007; revised 11 Jun 2007; accepted 11 Jun 2007; published 15 Aug 2007

The convergence study is subtle since the dependence on different parameters changes markedly with the region of parameter space. This occurs because at the peak of the quality factor curves, the dominant loss changes from in-plane to out-of-plane. The computation of Q is in general more sensitive at very large Qs. This can be seen in the data in Tables 1-3 which illustrates the influence of Δx at the maximum of $Q(f)$ for different structures.

Table 1. Evolution of frequency v and quality factor Q with grid resolution for a V_2^2 cavity at $f = 0.48$.

$a/\Delta x$	v	Q factor
16	0.31112426	6.5401e+06
20	0.31176333	5.8682e+06
24	0.31206435	5.7867e+06
32	0.31234943	5.5713e+06

Table 2. Evolution of frequency v and quality factor Q with grid resolution for a V_1^2 cavity at $f = 0.52$.

$a/\Delta x$	v	Q factor
16	0.30831709	1.1930e+06
20	0.30894683	1.2602e+06
24	0.30923272	1.2274e+06
32	0.30952279	1.2371e+06

Table 3. Evolution of frequency v and quality factor Q with grid resolution for a V_5^2 cavity at $f = 0.44$.

$a/\Delta x$	v	Q factor
16	0.31214530	1.0921e+07
20	0.31285747	1.0381e+07
24	0.31314226	1.1466e+07
32	0.31344269	1.1120e+07

The final set of parameters used for most calculations was $\Delta x = a/16$, $z_{\max} = 2a$, $w_{PML} = a$, $\Delta t = \Delta x/2$. The longest simulation runs typically used 2^{16} or 2^{17} timesteps. These values represent a compromise between high accuracy and the ability to perform a very large number of 3D calculations. We established that these parameters gave an accuracy (relative difference between calculations done with $\Delta x = a/16$ and $\Delta x = a/32$) in Q of better than 20% over all structures. Away from the peaks, the accuracy in Q is of the order of 1–3%. Finally, even at the peaks where the inaccuracies are expected to be largest, we checked that the location of the peaks did not change significantly with the chosen parameters than with the converged values at finer grid densities and larger vertical domain.

B. Influence of the number of adaptation layers

We considered mainly cavities with two adaptation layers. The reason was twofold. First, using two adaptation layers results in a large enough confinement for most practical applications. Second, we wanted to keep the design as simple as possible from the standpoint of fabrication

#82387 - $15.00 USD Received 24 Apr 2007; revised 11 Jun 2007; accepted 11 Jun 2007; published 15 Aug 2007

techniques. Indeed, using many adaptation layers would require to accommodate minute adjustments on the hole radius during the fabrication process. Nevertheless, for completeness we show in (Fig. 9) the evolution of the quality factor versus the number j of adaptation layers for a V_2^j cavity. Note that while the mode volume (not shown) increases with the number of layers, it does so slowly enough to ensure that Q/V increases monotonically.

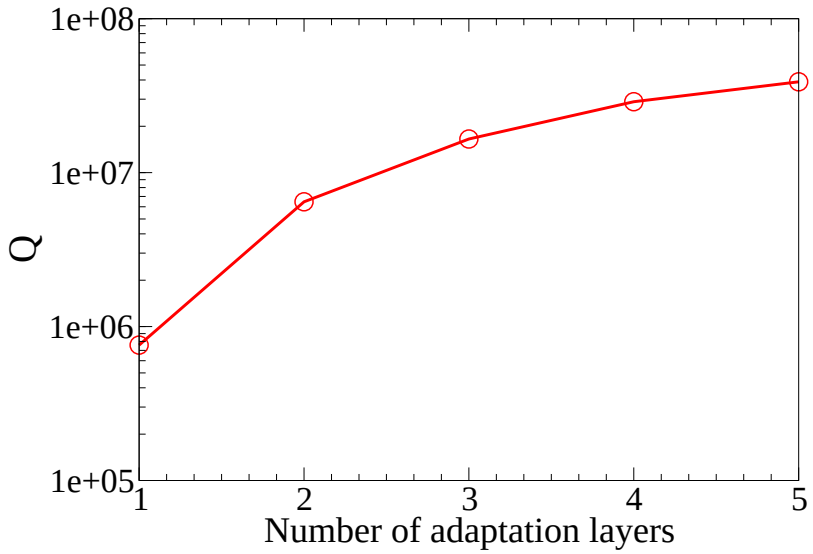

Fig. 9. Quality factor vs. the number j of adaptation layers for V_2^j cavities for a filling factor of the core $f_{\text{core}} = 0.48$.

#82387 - $15.00 USD Received 24 Apr 2007; revised 11 Jun 2007; accepted 11 Jun 2007; published 15 Aug 2007